

## Adsorbed Oxygen Species Formed by the Decomposition of $N_2O$ on Li/MgO Catalysts

Masato NAKAMURA, Hiroshi YANAGIBASHI, Hiroyuki MITSUHASHI, and Nobutsune TAKEZAWA\*

Department of Chemical Process Engineering, Hokkaido University, Sapporo 060

(Received February 18, 1993)

A considerable amount of adsorbed oxygen species were produced by the decomposition of  $N_2O$  on Li/MgO. The amount of the oxygen species greatly increases by Li(I)-doping on MgO. Over 0.7 wt% Li/MgO, the amount of the oxygen species formed was  $10.67 \mu\text{mol m}^{-2}$ . The temperature-programmed desorption of the oxygen species revealed that two types of adsorbed oxygen species were present on Li/MgO; one ( $\alpha$ -oxygen species) desorbed in proportion to the second order in the amount of the adsorbed species with an activation energy of  $141 \text{ kJ mol}^{-1}$ , giving a peak ( $\alpha$ -oxygen peak) at 673–693 K; the other ( $\beta$ -oxygen species) desorbed in proportion to the first order in the amount of the adsorbed species with an activation energy of  $219 \text{ kJ mol}^{-1}$ , giving a peak ( $\beta$ -oxygen peak) at 753–768 K. A weak  $\alpha$ -oxygen peak occurred on MgO and no  $\beta$ -oxygen peak was discerned. On Li/MgO, a  $\beta$ -oxygen peak appeared along with an  $\alpha$ -oxygen peak. At higher Li-loadings the  $\beta$ -oxygen peak was more intense than the  $\alpha$ -oxygen peak. The sites for these oxygen species were suggested to be derived by the addition of Li(I) on MgO. It was suggested that the  $\alpha$ -oxygen species were present at the surface sites on higher index faces of MgO, whereas the  $\beta$ -oxygen species were present at oxygen vacancies in the vicinity of Li(I) substituting for Mg(II). The hydrolysis of these adsorbed oxygen species yielded an appreciable amount of  $H_2O_2$ , suggesting that these species were primarily present as surface peroxide on MgO and Li/MgO.

It has been shown<sup>1,2)</sup> that Li/MgO catalysts are highly effective for the oxidative coupling of methane. Molecular oxygen is adsorbed on Li/MgO, forming the  $O^-$  species. These oxygen species react with  $CH_4$ , giving methyl radicals which undergo a coupling reaction to ethane and ethene. When  $N_2O$  was used in place of molecular oxygen, the coupling reaction also occurred in high selectivity.<sup>3,4)</sup> The oxygen species formed by the decomposition of  $N_2O$  were suggested to be involved in the oxidative coupling of methane.

The present study was aimed at an elucidation of the natures and the surface sites of adsorbed oxygen species formed by the decomposition of  $N_2O$  on Li/MgO with the help of the temperature-programmed desorption (TPD) method. By the hydrolysis of adsorbed oxygen species the presence of surface peroxide species was suggested.

### Experimental

The catalysts used were Li/MgO with 0.09, 0.23, 0.46, 0.58, and 0.70 wt% Li (the weight percentage is defined as ratio of Li(I) to sum of Li(I) plus MgO) and an unpromoted MgO. Li/MgO was prepared by impregnation of MgO in a given concentration of a solution of LiOH (Wako Chemicals Ltd., extra pure grade) at room temperature and dried at 383 K overnight. MgO (Wako Chemicals Ltd., extra pure grade) was prepared after being soaked in distilled water and dried at 383 K overnight. Thus-obtained Li/MgO and MgO samples were packed in reactors, and heated at 1073 K for 3 h in a stream of  $O_2$  (20 vol%). The  $O_2$  stream was then switched to that of helium, and the reactor was cooled to temperatures at which the  $N_2O$  decomposition ( $P_{N_2O}=15.2 \text{ kPa}$ ) or the  $O_2$  adsorption ( $P_{O_2}=15.2 \text{ kPa}$ ) was conducted at a flow rate of  $150 \text{ cm}^3 \text{ min}^{-1}$ . Helium was used as a diluent.

TPD runs were conducted at heating rates of 2–20

$\text{K min}^{-1}$  in a helium flow of  $30 \text{ cm}^3 \text{ min}^{-1}$ . Gases from the reactor were collected every 3 min in a sampling tube attached to the outlet of the reactor for analysis. The experiments were repeatedly conducted under given conditions, and the reproducibility of the TPD curves was confirmed.

All of the gases used were purified by passage through a trap cooled at 195 K in dry ice-methanol. The gas compositions in the effluent were determined by a gas chromatograph with a thermal conductivity detector. For the analysis of  $H_2O_2$ , the Ti(IV) species was used as an indicator,<sup>5,6)</sup> and the UV-vis spectra of the spectrophotometer (Hitachi 330). The surface areas of the catalysts (Table 1) were determined by the BET method.

### Results and Discussion

**TPD of Adsorbed Oxygen Species.** The decomposition of  $N_2O$  occurred at temperatures above 523 K over Li/MgO and MgO, giving  $N_2$  and  $O_2$ . During the initial period of the decomposition of  $N_2O$ , the response of  $O_2$  is markedly different from that of  $N_2$ . The partial pressure of  $O_2$  slowly increases to a steady state value, whereas that of  $N_2$  overshoots within 10 s, and then decreases. Under the transient state of the reaction, the partial pressure of  $N_2$  in the effluent exceeded that of the expected  $O_2$  based on the stoichiometry of the decomposition of  $N_2O$ . This reasonably suggests

Table 1. Surface Area of Li/MgO

wt% Li	Surface area ( $\text{m}^2/\text{g-catalyst}$ )
0	102
0.09	78.0
0.23	63.7
0.46	21.3
0.58	2.8
0.70	2.0

that the adsorbed oxygen species are formed on Li/MgO during the course of  $\text{N}_2\text{O}$  decomposition.

Figure 1 illustrates the TPD profiles obtained after the  $\text{N}_2\text{O}$  decomposition was carried out over 0.46 wt% Li/MgO for various time periods. Under the present experimental conditions, since the conversion of  $\text{N}_2\text{O}$  was always lower than 1.6%, the partial pressure of  $\text{N}_2\text{O}$  was practically constant throughout the catalyst bed in the decomposition of  $\text{N}_2\text{O}$ . For a catalyst subjected to the decomposition of  $\text{N}_2\text{O}$  for shorter periods of time, one peak of  $\text{O}_2$  desorption occurs at 750 K ( $\beta$ -oxygen peak). During the course of TPD runs, no other species were detected in the effluent. Unless  $\text{N}_2\text{O}$  was previously decomposed, no  $\text{O}_2$  desorption occurred during the TPD runs. For a catalyst subjected to the decomposition of  $\text{N}_2\text{O}$  for longer periods of time, the intensity of the  $\beta$ -oxygen peak increases, and a new  $\text{O}_2$  desorption peak ( $\alpha$ -oxygen peak) is discernible at around 673 K on a shoulder of  $\beta$ -oxygen peak. The total amount of  $\text{O}_2$  desorbed was estimated from the peak area. For the catalyst previously subjected to  $\text{N}_2\text{O}$  decomposition at 573 K for 2 h, the total amount of desorbed oxygen was estimated to be  $2.7 \mu\text{mol m}^{-2}$  catalyst. On the basis of the BET surface area, this corresponds to about 14.5 or 29% of the surface of the catalyst, based on the assumption that the catalyst surface was exposed to the (100) faces of MgO, and that the adsorbed species were in their molecular or atomic forms.

When 0.46 wt% Li/MgO was subjected to molecular oxygen exposure for 1 h, a very weak peak of the des-

orption of  $\text{O}_2$  was discerned at 745 K in TPD runs, and was ascribable to the  $\beta$ -oxygen peak. The total amount of desorbed oxygen was estimated to be  $2.2 \times 10^{-2} \mu\text{mol m}^{-2}$  of catalyst. In a similar manner, TPD was carried out over MgO previously exposed to molecular oxygen. No oxygen was desorbed. Hence, we concluded that the amount of the oxygen species formed by the adsorption of molecular oxygen was practically negligible, as compared with that formed in the decomposition of  $\text{N}_2\text{O}$  over Li/MgO and MgO. The adsorbed oxygen species were formed through the decomposition of  $\text{N}_2\text{O}$  before desorbing in the gaseous phase.

Figure 2 illustrates the relationship between the amount of adsorbed oxygen species evolved during the TPD runs and that estimated on the basis of the response curves of  $\text{N}_2$  and  $\text{O}_2$  in the transient state of the decomposition of  $\text{N}_2\text{O}$  over 0.46 wt% Li/MgO. The former value is in good agreement with the latter value, strongly suggesting that all of the adsorbed oxygen species formed during the decomposition of  $\text{N}_2\text{O}$  were desorbed during TPD runs.

Figure 3 illustrates the TPD profiles obtained after the decomposition of  $\text{N}_2\text{O}$  was carried out at 573 K for 1 h over MgO and various Li/MgO catalysts. Over MgO, one weak peak appears at 690 K and is ascribed to the  $\alpha$ -oxygen peak. No  $\beta$ -oxygen peak occurs. The amount of  $\text{O}_2$  desorbed was estimated to be  $0.03 \mu\text{mol m}^{-2}$  of catalyst, corresponding to only 0.15 or 0.3% of the surface based on the assumption that the adsorbed oxygen species are either molecular or atomic. Over Li/MgO, the  $\beta$ -oxygen peak occurs in addition to the  $\alpha$ -oxygen

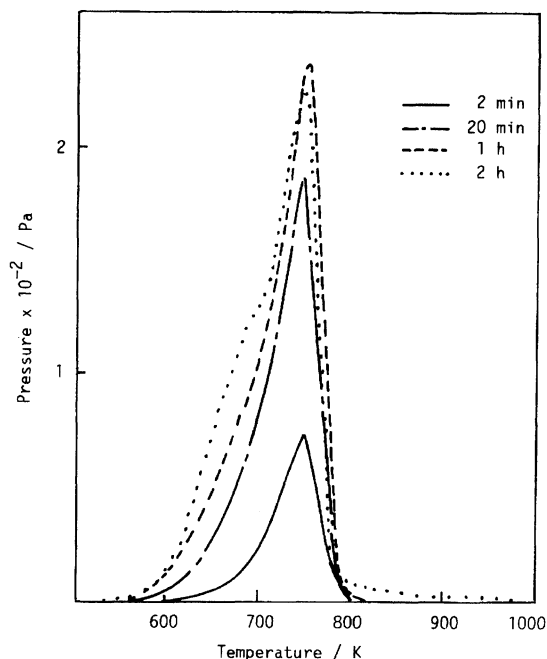


Fig. 1. TPD profiles of oxygen formed by a reaction with  $\text{N}_2\text{O}$  over 0.46 wt% Li/MgO.  $\text{N}_2\text{O}$  decomposition was carried out at 573 K for various periods of time described in the figure.

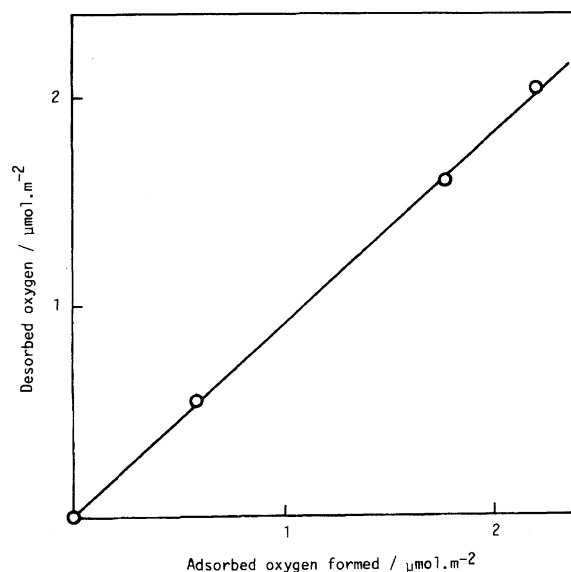


Fig. 2. Relationship between the amount of adsorbed oxygen species evolved in TPD runs and that estimated from the response curves of  $\text{N}_2$  and  $\text{O}_2$  in the effluent in the transient state of the  $\text{N}_2\text{O}$  decomposition.  $\text{N}_2\text{O}$  decomposition was carried out at 573 K and at an inlet pressure of  $\text{N}_2\text{O}$  of 15.2 kPa.

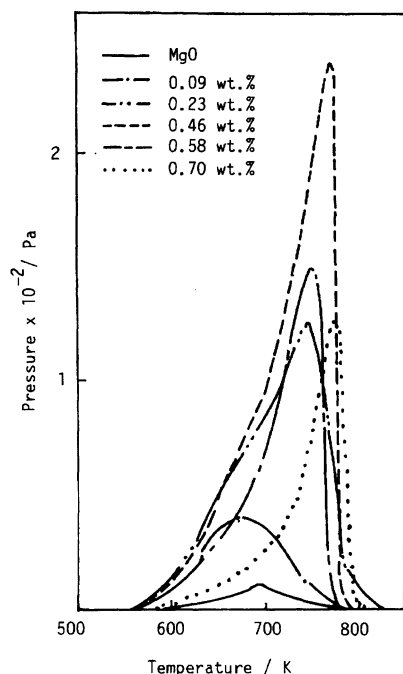


Fig. 3. TPD profiles of oxygen formed by the decomposition of  $N_2O$  over various Li/MgO. The  $N_2O$  decomposition was carried out at 573 K for 1 h at an inlet partial pressure of  $N_2O$  of 15.2 kPa.

peak. Upon increasing the amount of Li-loading up to 0.46 wt%, the intensities of these peaks increases markedly. For catalysts having higher Li-loadings the intensity of the  $\beta$ -oxygen peak is more appreciable than that of the  $\alpha$ -oxygen peak.

**Simulation of TPD Profiles and Surface Sites for Adsorbed Oxygen Species.** As shown above, two desorption peaks of  $O_2$  occurred over Li/MgO in the TPD runs. The separation of these peaks was incomplete for desorption over 0.09, 0.23, 0.46, and 0.58 wt% Li/MgO. On the other hand, over MgO one peak ascribed to the desorption of the  $\alpha$ -oxygen species appeared. Over 0.70 wt% Li/MgO, the  $\beta$ -oxygen peak predominates, as judged from the TPD profile. It can be safely assumed that the position of the  $\beta$ -oxygen peak is practically unaffected by the presence of the  $\alpha$ -oxygen species. The activation energy ( $E_d$ ), and desorption order ( $n$ ) for the  $\alpha$ - and  $\beta$ -oxygen species were first estimated from the TPD profiles obtained over MgO and 0.70 wt% Li/MgO, respectively. These estimated parameters were adopted for a simulation of TPD profiles for the  $\alpha$ - and  $\beta$ -oxygen species over other Li/MgO catalysts.

Cvetanovic and Amenomiya<sup>7)</sup> as well as Kojima et al.<sup>8)</sup> previously showed that the relationship

$$\ln(T_m^2/g) = E_d/RT_m + \ln E_d/(nRk_oN_m^{n-1}) \quad (1)$$

exists for desorption during the TPD runs in which the temperature ( $T$ ) increases from  $T_0$  linearly with time ( $t$ )

as  $T = T_0 + gt$ , where  $T_m$  is the peak temperature,  $g$  the heating rate,  $k_o$  the frequency factor of the desorption, and  $N_m$  the amount of adsorbed species at the peak temperature. When the heating rate is varied at a given  $N_m$ , the value of  $\ln(T_m^2/g)$  obtained can be a linear function with respect to  $1/T_m$ . The  $E_d$ -value is thus estimated from the slope of the line. When the amount of preadsorbed oxygen is varied at a given  $g$ , the value of  $\ln(T_m^2) - E_d/RT_m$  can be expressed as a linear function with respect to  $\ln N_m$ . The slope of the line gives the  $(1-n)$ -value.

Figure 4 illustrates the relationship between  $\ln(T_m^2/g)$  and  $1/T_m$  at  $N_m = 3.23 \mu\text{mol m}^{-2}$  of catalyst over 0.70 wt% Li/MgO. A good linear relationship exists. From the slope of the line, the activation energy of the desorption was estimated to be 219 kJ mol<sup>-1</sup>. In Fig. 5, a plot between  $\ln(T_m^2) - E_d/RT_m$  and  $\ln N_m$  is illustrated at  $g = 7 \text{ K min}^{-1}$ , at which the amount of the preadsorbed oxygen species was varied. The values of the ordinate are practically independent of  $\ln N_m$ , indicating that the desorption of oxygen is of the first order regarding the amount of the adsorbed oxygen species. In a similar manner, the activation energy of the desorption and desorption order were determined over MgO. From the respective plots given in Figs. 6 and 7, we concluded that the activation energy is 141 kJ mol<sup>-1</sup> and that the desorption proceeds in proportion to the second order regarding the amount of adsorbed species.

On the basis of the activation energies and desorption orders thus estimated for the  $\alpha$ - and  $\beta$ -oxygen species, the TPD profiles for these oxygen species were determined for samples with various Li-loadings. The TPD profile obtained by superimposing the estimated  $\alpha$ -oxygen and  $\beta$ -oxygen peaks was compared with the ob-

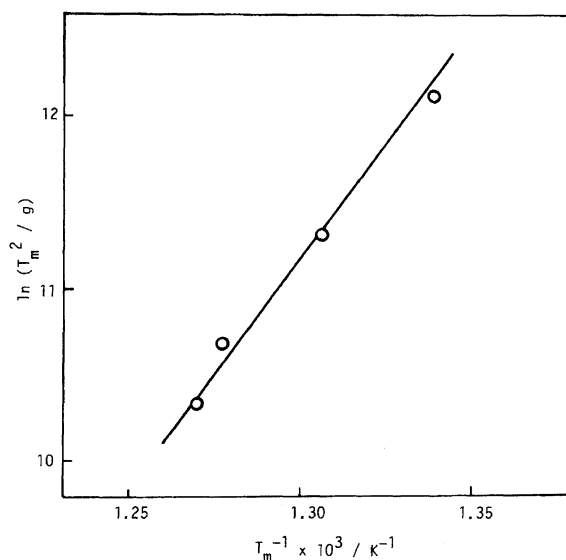


Fig. 4. Relationship between  $\ln(T_m^2/g)$  and  $1/T_m$  for 0.70 wt% Li/MgO. The amount of adsorbed oxygen species ( $N_m$ ) was  $3.23 \mu\text{mol m}^{-2}$ .

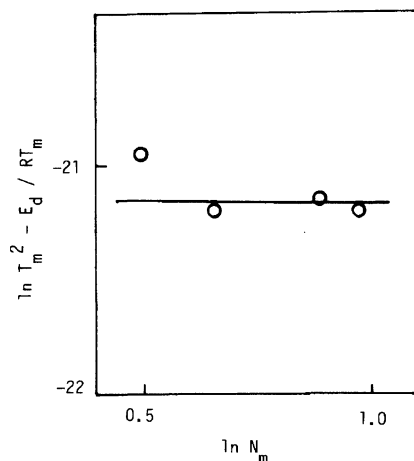


Fig. 5. Relationship between  $\ln(T_m^2) - E_d/RT_m$  and  $\ln N_m$  for 0.70 wt% Li/MgO. The rate of the temperature rise ( $g$ ) was  $7 \text{ K min}^{-1}$ .

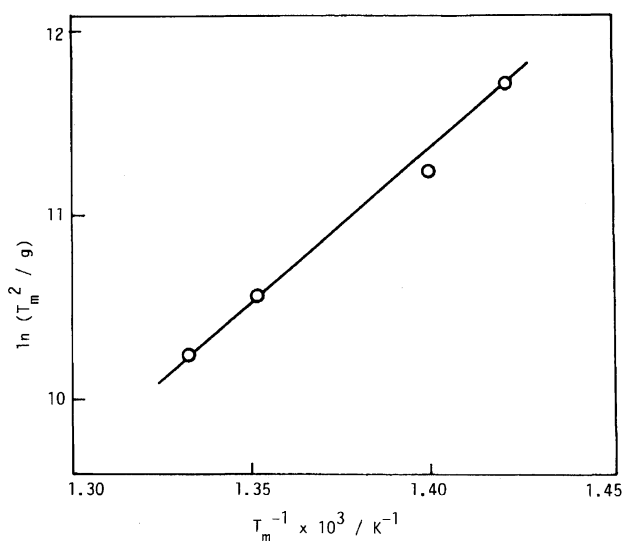


Fig. 6. Relationship between  $\ln(T_m^2/g)$  and  $1/T_m$  for MgO. The amount of adsorbed oxygen species ( $N_m$ ) was  $5.7 \times 10^{-3} \mu\text{mol m}^{-2}$ .

served profile. Figure 8 illustrates the TPD profile thus obtained for 0.46 wt% Li/MgO. The simulated peak agreed with the observed peak.

Figure 9(a) illustrates the amounts of  $\alpha$ - and  $\beta$ -oxygen species determined by a simulation of TPD profiles against the Li-loading. The amounts of  $\alpha$ - and  $\beta$ -oxygen species increase up to 0.3 and 0.46 wt% Li, respectively and decrease with increasing Li-loading. As opposed to the decrease of the surface area of the samples (Table 1), the amount of  $\alpha$ -oxygen species present on 0.23 wt% Li/MgO is 8 times as much as that present on MgO. As evident from the figure, the  $\beta$ -oxygen species emerge upon the addition of Li(I) on MgO. Figure 9(b) gives a plot of the amount of adsorbed oxygen species based on the surface area against the Li-loading. It shows the surface concentration of the  $\alpha$ - and  $\beta$ -oxygen

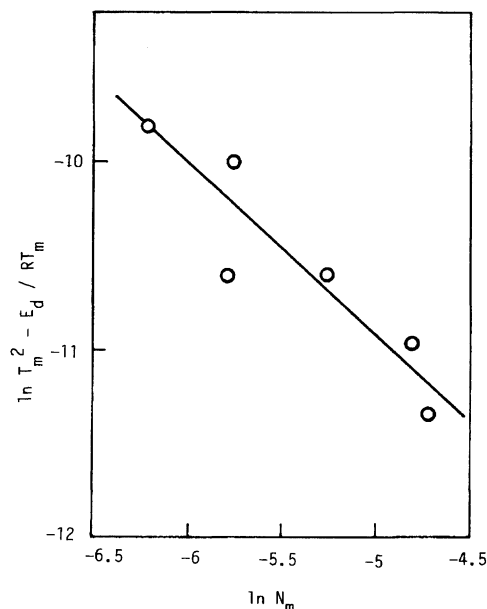


Fig. 7. Relationship between  $\ln(T_m^2) - E_d/RT_m$  and  $\ln N_m$  for MgO. The rate of the temperature rise ( $g$ ) was  $7 \text{ K min}^{-1}$ .

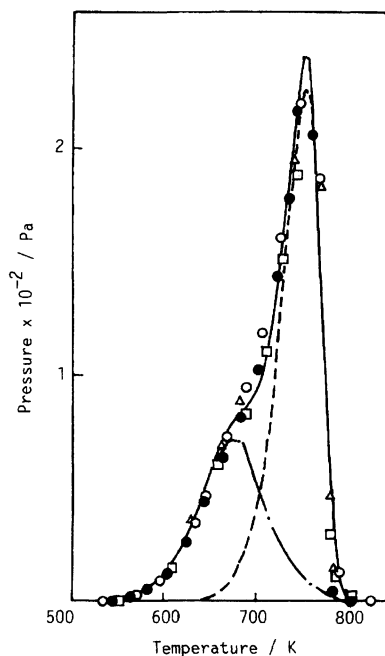


Fig. 8. Calculated TPD profile vs observed TPD profile. Catalyst, 0.46 wt% Li/MgO: Amount of adsorbed oxygen species =  $2.25 \mu\text{mol m}^{-2}$  catalyst. TPD runs were repeatedly conducted. The marks  $\circ$ ,  $\bullet$ ,  $\triangle$ , and  $\square$  represent the results obtained in different TPD runs. —, calculated TPD profile for the sum of  $\alpha$ - and  $\beta$ -oxygen species; ---, calculated TPD profile for  $\alpha$ -oxygen species; - · -, calculated profile for  $\beta$ -oxygen species.

species increased with increased Li-loading. The total surface concentration of these adsorbed species reached

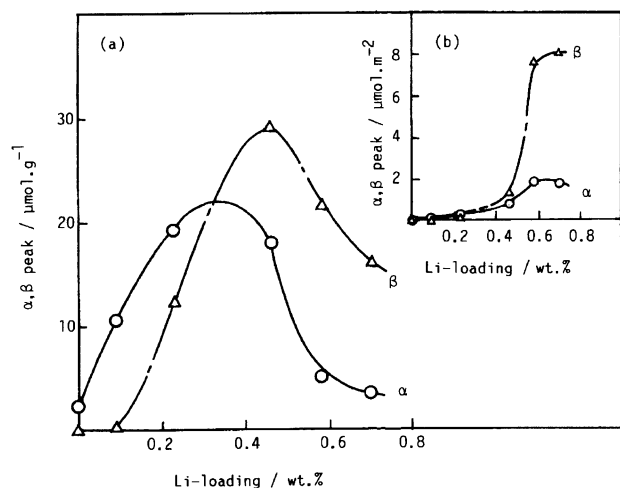


Fig. 9. (a) Amounts of  $\alpha$ - and  $\beta$ -oxygen species per gram of catalyst versus Li-loading. (b) Amounts of  $\alpha$ - and  $\beta$ -oxygen species per m<sup>2</sup> of catalyst surface versus Li-loading.

10.67  $\mu\text{mol m}^{-2}$  over 0.70 wt% Li/MgO, being as much as 57 or 114% of the catalyst surface, based on the assumption that the adsorption was either in molecular or atomic form. Hence, the surface sites for the oxygen species were generated by doping with Li(I).

It has been shown that the Mg(II) sites are partly replaced by Li(I) for MgO doped with Li(I), and that oxygen vacancies are generated.<sup>1,2,9-11</sup> Hargreaves et al.<sup>12</sup> recently studied the morphologies of Li/MgO using transmission electron microscopy, showing that the addition of Li(I) causes a loss of the surface area as well as the morphology characteristics of MgO. The grain size of MgO increases. Dislocations in the grain boundary and in the bulk of the grains emerged, probably providing oxygen vacancies close to the Li(I) in MgO. In addition, MgO particles having cubic structures ((100) faces predominantly exposed) were deformed to quasi-spherical structures for MgO doped with Li(I), suggesting that higher index crystal faces were generated on the MgO surface. Since adsorbed oxygen species were probably formed on these sites, the amounts of these species increased markedly upon the Li(I)-doping on MgO. The Mg(II) sites located on the higher index faces, i.e. sites with lower coordination numbers, would be present on MgO to some extent, and thus responsible for the formation of the  $\alpha$ -oxygen species. On the other hand, since  $\beta$ -oxygen species appeared on MgO doped with Li(I), these adsorbed species would be captured in oxygen vacancies which are probably located in the vicinity of Li(I) substituting for Mg(II).

**States of the Adsorbed Oxygen Species and the Mechanism for the Formation of Adsorbed Oxygen Species.** MgO and Li/MgO samples containing adsorbed oxygen species was soaked in a solution of sulfuric acid and the formation of H<sub>2</sub>O<sub>2</sub> were tested by using Ti(IV) as an indicator. A strong absorp-

tion ascribed to the peroxotitanium(IV) species occurs at 407 nm in the UV spectra of the solution (Fig. 10). Unless adsorbed oxygen species are present on the surface, no absorption occurs at 407 nm. In Fig. 11, the amount of H<sub>2</sub>O<sub>2</sub> formed is plotted against that of the adsorbed oxygen species on the basis of the results for the samples shown in Fig. 10. It shows that the amount of H<sub>2</sub>O<sub>2</sub> species is practically the same as that of the oxygen species present on MgO and Li/MgO. The adsorbed oxygen species were, therefore, most probably present as surface peroxide and hydrolyzed to H<sub>2</sub>O<sub>2</sub> through  $\text{MgO}_2 + 2\text{H}_2\text{O} \rightarrow \text{Mg}(\text{OH})_2 + \text{H}_2\text{O}_2$  and  $\text{Li}_2\text{O}_2 + 2\text{H}_2\text{O} \rightarrow 2\text{LiOH} + \text{H}_2\text{O}_2$  reactions in a sulfuric acid solution as various alkali and alkaline earth metal peroxides were hydrolyzed.<sup>13-15</sup>

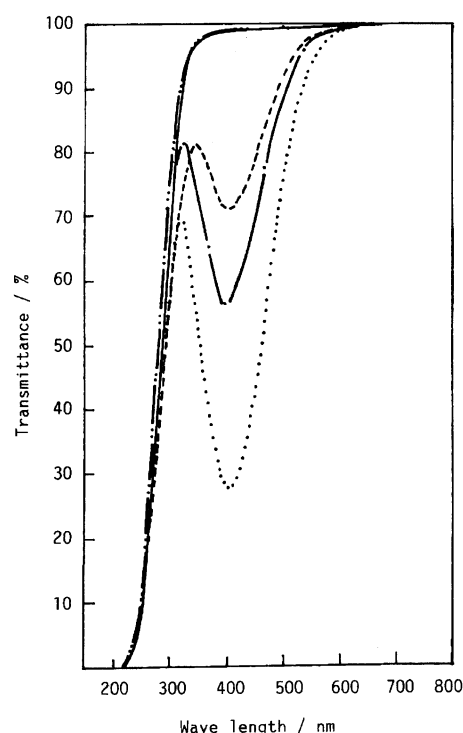


Fig. 10. UV-vis spectra of peroxotitanium(IV) species formed by reaction between Ti(IV) and H<sub>2</sub>O<sub>2</sub> formed by hydrolysis of adsorbed oxygen species in a sulfuric acid solution.

---, 0.46 wt% Li/MgO; sample weight=0.69 g. Adsorbed oxygen species were absent. Ti(IV) solution used=50 cm<sup>3</sup>.

—, MgO; sample weight=0.69 g. Adsorbed oxygen species were absent. Ti(IV) solution used=20 cm<sup>3</sup>.

---, MgO; sample weight=0.69 g. The amount of adsorbed oxygen species=2.04  $\mu\text{mol}$ . Ti(IV) solution used=20 cm<sup>3</sup>.

...., 0.46 wt% Li/MgO; sample weight=0.69 g. The amount of adsorbed oxygen species=33.1  $\mu\text{mol}$ . Ti(IV) solution used=50 cm<sup>3</sup>.

-.-., 0.70 wt% Li/MgO; sample weight=0.69 g. The amount of adsorbed oxygen species=14.7  $\mu\text{mol}$ . Ti(IV) solution used=50 cm<sup>3</sup>.

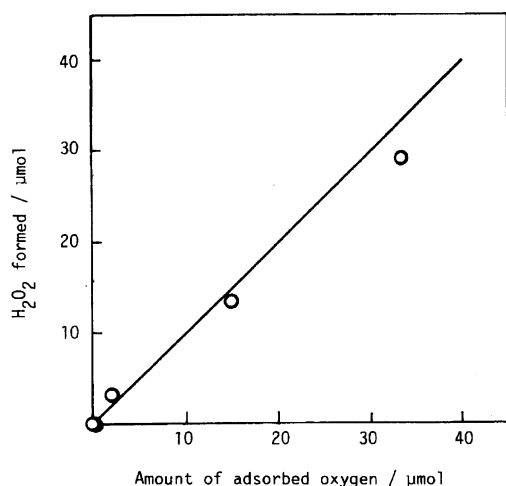


Fig. 11. Amount of  $\text{H}_2\text{O}_2$  formed vs amount of adsorbed oxygen species formed by the decomposition of  $\text{N}_2\text{O}$ .

It has been reported that the O–O bond is ruptured during the decomposition of alkali and alkaline earth metal peroxide by the use of the  $\text{O}^{18}$  isotope.<sup>16–18)</sup> Hence, the dissociation of the O–O bond is probably involved in the decomposition of the surface peroxide species. Ito et al.<sup>19)</sup> as well as Cordischi et al.<sup>20)</sup> previously suggested that the surface peroxide species decompose through a bimolecular reaction. On the basis of the observed desorption kinetics, the  $\alpha$ -oxygen species would desorb through this process. However, it is also probable that surface peroxide species are dissociated through a  $\text{O}_2^{2-} \rightarrow 2\text{O}^-$  step.<sup>21)</sup> Based on the condition that the surface oxygen species are predominantly transformed to  $\text{O}^-$  species prior to desorption, the desorption also obeys second-order kinetics. In contrast, based on the condition that the dissociation step,  $\text{O}_2^{2-} \rightarrow 2\text{O}^-$ , is rate determining, the desorption of oxygen proceeds in proportion to the first order in the amount of surface oxygen species. This would be the case for the desorption of  $\beta$ -oxygen species.

In the present work, we showed that a considerable amount of adsorbed oxygen species was formed in the decomposition of  $\text{N}_2\text{O}$ . The amount of the oxygen species was extremely large compared with that of adsorbed oxygen species formed by the adsorption of molecular oxygen. Over  $\text{MgO}$  the decomposition of  $\text{N}_2\text{O}$  proceeded at a rate proportional to the partial pressure of  $\text{N}_2\text{O}$  at the steady state of the reaction, whereas over  $\text{Li/MgO}$  the desorption proceeded at a rate proportional to the 0.5th order in that of  $\text{N}_2\text{O}$ . Over these catalysts the decomposition of  $\text{N}_2\text{O}$  were unaffected by the presence of molecular oxygen. These findings suggested that the desorption of oxygen was

irreversible in the decomposition of  $\text{N}_2\text{O}$ . Under such conditions, the chemical potential of the adsorbed oxygen species greatly exceeded that of molecular oxygen in the gaseous phase. This gave rise to a great increase in the virtual pressure of the adsorbed oxygen species. Hence, the formation of adsorbed oxygen was more favorable in the decomposition of  $\text{N}_2\text{O}$ , rather than in the adsorption of molecular oxygen.

## References

- 1) T. Ito, J.-X. Wang, C.-H. Lin, and J. H. Lunsford, *J. Am. Chem. Soc.*, **107**, 5062 (1985).
- 2) D. J. Driscoll, W. Matir, J.-X. Wang, and J. H. Lunsford, *J. Am. Chem. Soc.*, **107**, 58 (1985).
- 3) J. Cunningham and D. McNamara, *Catal. Today*, **6**, 551 (1990).
- 4) M. Nakamura, H. Mitsuhashi, and N. Takezawa, to be published.
- 5) H. Pobine, *Anal. Chem.*, **33**, 1423 (1961).
- 6) C. C. Winterbourn, R. C. Garcia, and A. W. Segal, *Biochem. J.*, **228**, 583 (1985).
- 7) R. J. Cvetanovic and Y. Amenomiya, "Advances in Catalysis," ed by D. D. Eley, H. Pines, and P. B. Weisz, Academic Press, New York (1967), Vol. 17, p.1-3.
- 8) I. Kojima, M. Komiyama, and I. Yasumori, *Bull. Chem. Soc. Jpn.*, **53**, 2123 (1980).
- 9) Y. Chen, H. T. Tohver, J. Narajan, and M. M. Abram, *Phys. Rev. Sect. B*, **16**, 5535 (1977).
- 10) J. B. Lacy, M. M. Abram, O. J. L. Bolodu, Y. Chen, J. Narajan, and H. T. Tohver, *Phys. Rev. Sect. B*, **18**, 4136 (1978).
- 11) O. J. L. Bolodu, M. M. Abram, and Y. Chen, *Phys. Rev. Sect. B*, **19**, 4421 (1979).
- 12) J. S. J. Hargreaves, G. J. Hutchings, R. W. Joyner, and C. J. Kiely, *J. Catal.*, **135**, 576 (1992).
- 13) M. Nakamura, S. Fujita, and N. Takezawa, *Catal. Lett.*, **14**, 315 (1992).
- 14) J. W. Mellor, "Comprehensive Treatise on Inorganic and Theoretical Chemistry," Longmans, London (1960), Vol. 3.
- 15) "Encyclopedia Chimica," ed by S. Mizushima, Kyoritsu Pub. Co., Tokyo (1960), Vol. 2.
- 16) V. Z. Kuprii and V. A. Lunenok-Burmakina, *J. Phys. Chem. (Moscow)*, **45**, 101 (1971).
- 17) V. A. Lunenok-Burmakina and V. Z. Kuprii, *J. Inorg. Chem. USSR*, **16**, 2331 (1971).
- 18) V. Z. Kuprii and V. A. Lunenok-Burmakina, *J. Phys. Chem. (Moscow)*, **45**, 179 (1971).
- 19) T. Ito, M. Kato, K. Toi, T. Shirakawa, I. Ikemoto, and T. Tokuda, *J. Chem. Soc., Faraday Trans. 1*, **81**, 2835 (1985).
- 20) V. Indovina and D. Cordischi, *J. Chem. Soc., Faraday Trans.*, **78**, 1705 (1982).
- 21) H. Yamashita, Y. Machida, and A. Tomita, *Appl. Catal.*, **79**, 203 (1991).